Precipitation Analysis Using AMSU and AVHRR Data in Support of Nowcasting Applications

Ralf Bennartz, FU Berlin, Germany

Anke Thoss, Adam Dybbroe, Daniel Michelson, SMHI Sweden

1. Introduction

Within the framework of the EUMETSAT Satellite Application Facility to support Nowcasting and very short range forecasting, SMHI is developing four cloud products from AVHRR and AMSU data: Cloud Mask, Cloud Type, Cloud Top Temperature and Height and Precipitating Cloud. The Precipitating Cloud (PC) product is described in this paper.

The requirements of a nowcasting precipitation product differ in some aspects from the precipitation products in climate research. Whereas climate products need a high absolute accuracy to detect climate signals, but employ temporal and spatial averaging, a nowcasting product should employ the best possible spatial resolution. On the other hand the absolute accuracy of precipitation amount is not of major importance. In our case we found the definition of four intensity classes sufficient. The precipitation is specified as the likelihood of precipitation in each intensity class. Another major requirement on a nowcasting product is the timely generation for the region of interest.

2. Development Dataset

The algorithm development was performed using an eight month dataset (April 1999 to November 1999) of NOAA-15 AMSU-A/B and AVHRR data. The data was co-located with radar data from the BALTEX Radar Data Centre (BRDC) for the entire Baltic region covered by 13 radars (Michelson et al, 2000). The precipitation amount of the radar data was gauge adjusted using a technique described in (Michelson and Koistinen, 2000).

3. Algorithm

The algorithm is giving the likelihood of precipitation in four intensity intervals under the constraint, that the total likelihood has to be 100%. Intensity classes are defined as follows:

Class 1:	Precipitation-free	rain rate 0.0 to 0.1 mm/h
Class 2:	Risk for or very light precipitation	rain rate 0.1 to 0.5 mm/h
Class 3:	Light/moderate precipitation	rain rate 0.5 to 5.0 mm/h
Class 4:	Intensive precipitation	rain rate greater 5.0 mm/h

Separate estimates of precipitation likelihood are performed from AMSU and AVHRR and finally blended into a joint estimate.

3.1 AMSU

Most information of the precipitation product is derived from microwave frequencies. When developing a precipitation algorithm for AMSU, we had to consider whether to concentrate on an emission or scattering based algorithm. Whereas the emission signal from precipitation for

frequencies below 50 GHz is more directly linked to precipitation, it can only be retrieved over water surfaces, which give a radiatively cold background because of their low surface emissivity. For frequencies higher than 50 GHz it is possible to derive precipitation algorithms based on the scattering signature of frozen precipitation sized particles over both land and sea (Bennartz and Petty, 2000). Since it was desirable to also make use of MW data over land, we developed a scattering based algorithm using AMSU-A and AMSU-B window channels. This enabled us to also take advantage of the higher spatial resolution of AMSU-B of 1.1° (corresponding to 16 km at nadir) as compared to AMSU-A with 3.3° resolution.

The scattering index makes use of a predicted brightness temperature T^* in the absence of scattering, which is derived from low frequency channels. The functional relationship between the low frequency brightness temperature and T^* can either be found by inverse radiative transfer modelling, or by global brightness temperature statistics. From T^* the high frequency brightness temperature is subtracted:

$$SI = T^*(T_{low}) - T_{high}$$

with SI being the scattering index, T_{low}, T_{high} being the observed low and high frequency brightness temperature respectively. The scattering index has been found to be a linear measure for precipitation intensity. In the algorithm described here, T^* is determined statistically as:

$$T^* = T_{low} - CORR$$

where CORR includes a statistical correction for scan position effects and a statistical offset for non-scattering situations. For algorithm development, it is necessary to take into account the surface properties of the scene viewed. Scene specifications will influence the channel selection and will also necessitate separate tuning of the correction coefficient. According to the scene viewed, our algorithm specifies three separate cases for FOV's covered with land or water:

- AMSU-A land (and AMSU-B land): $SI_{land1} = T23 - CORR - T150$
- AMSU-A water or coast, AMSU-B Land: $SI_{land2} = T89 - CORR - T150$
- AMSU-B water: $SI_{sea} = T89 - CORR - T150$

In the case of the water algorithm, the offset for non-scattering situations is adjusted dynamically for each scene processed.

Coastal estimates have to be treated separately. A linear dependence exists between the MW brightness temperatures and the land fraction within the FOV, as illustrated for the 23GHz channel in figure 1. Thus the scattering index for coastal scenes can be estimated as a linear combination of the land and sea scattering index, taking into account the land fraction within the FOV:

$$SI_{coast} = (1 - N_{land}) * SI_{sea} + N_{land} * SI_{land}$$

with N_{land} being the land fraction and SI_{land} and SI_{sea} being the scattering indices for land and sea respectively. Due to the high sensitivity of scene coverage within the FOV it is necessary to properly convolve a high resolution land/sea mask to the AMSU FOV, as well as to properly convolve AMSU-B to AMSU-A. We used a Backus-Gilbert convolution described by Bennartz (2000) for this purpose.

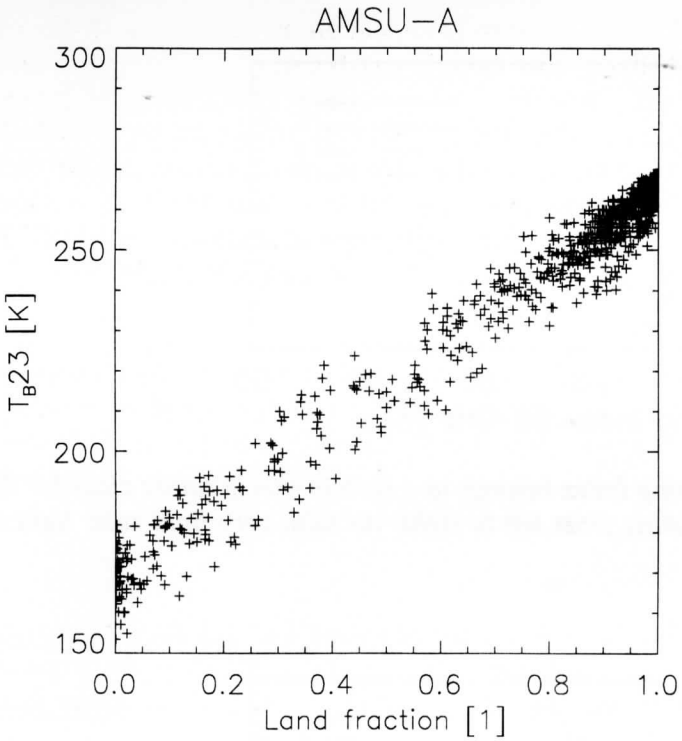

Figure 1: Dependence of AMSU-A brightness temperature at 23GHz on the fraction of land surface within the footprint.

The scattering indices are matched with gauge corrected radar rain rates, which have been convolved to the AMSU-B field of view. Frequency distributions of scattering indices have been derived for each of the four precipitation classes defined above. For each scattering index the probability that the observation falls within a certain precipitation class is determined under the constraint that the total probability has to sum up to 100%. It could be shown that the 23GHz-150GHz scattering index gives a better discrimination of precipitation over land than the 23GHz-89GHz scattering index (figures 2 and 3). The probability distribution of the scattering indices for the four precipitation classes is given in figure 3 for land and in figure 4 for sea. Whereas it is possible to clearly discriminate non-precipitating situations from strong precipitation, there is some overlap of the very light and the light/moderate precipitation classes with both the high and non-precipitation classes. The two intermediate classes overlap substantially with each other. In this light it seems even more valid, to express the precipitation estimate as probabilities.

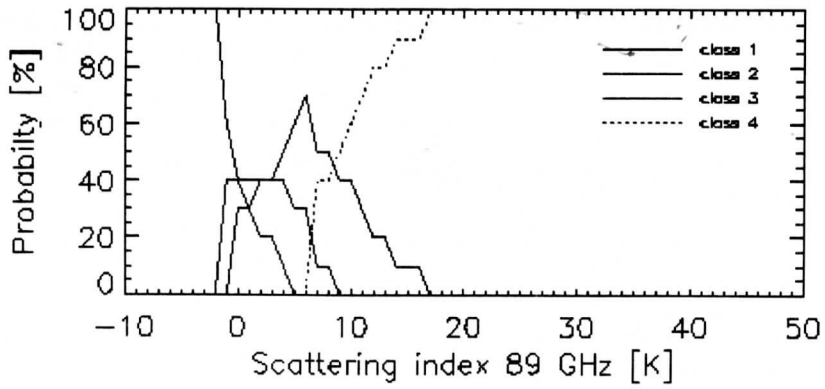

*Figure 2: Probability that the Scattering Index belongs to a certain precipitation class for the **23GHz-89GHz index over land**. Peaking from left to right: no rain, very light rain, light to moderate rain, heavy rain.*

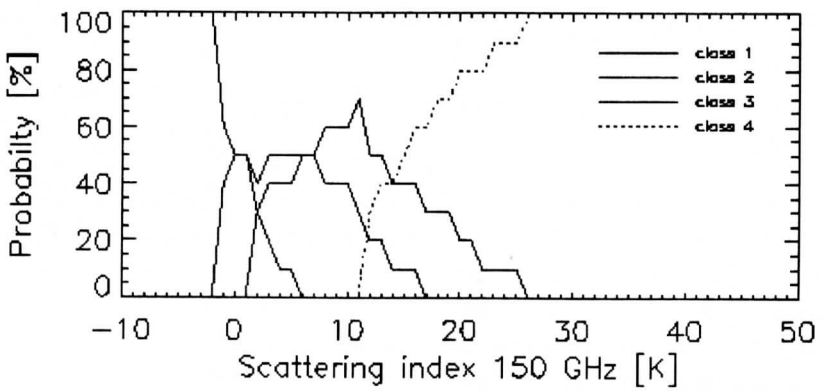

*Figure 3: Probability that the Scattering Index belongs to a certain precipitation class for the **23GHz-150GHz index over land**. Peaking from left to right: no rain, very light rain, light to moderate rain, heavy rain*

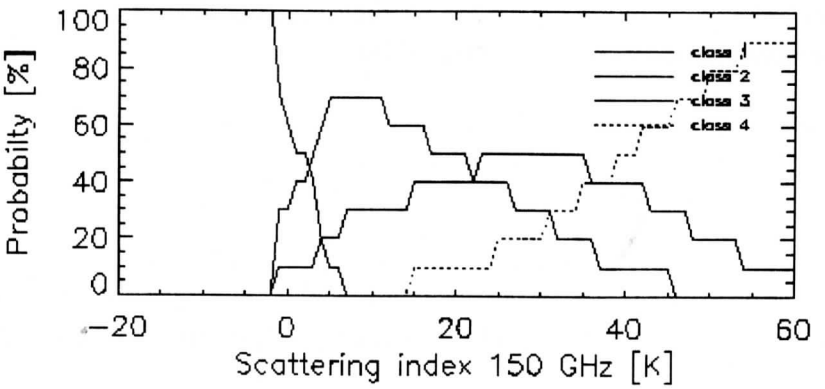

*Figure 4: Probability that the Scattering Index belongs to a certain precipitation class for the **89GHz-150GHz index over sea**. Peaking from left to right: no rain, very light rain, light to moderate rain, heavy rain*

3.2 AVHRR

At visible and infrared wavelengths, the coupling between spectral features and precipitation is much weaker as in the microwave region. Using radar data, we investigated the statistical coupling between spectral features in the AVHRR and precipitation. As expected, the 11 μm brightness temperature proved to be the most important feature. At day time, some additional information, specially with regard to intensity, can be derived from the reflectivity quota R0.6μ m/R3.7μ m. This feature is strongly influenced by micro-physical features at the cloud top, such as particle phase and size. The channel 3.7 μm reflectivity is derived using the 11 μm channel to correct for the thermal contribution. We constructed a day time Precipitation Index (PI) of the form:

$$PI_{day} = a * T_{surf} - b * T11 + c * \ln(R0.6 / R3.7)$$

with a,b and c being tunable coefficients, T_{surf} being the NWP surface temperature. At night time we add some correction for semi-transparency derived from the brightness temperature difference of AVHRR channels four and five to the 11 μm brightness temperature information:

$$PI_{night} = a * T_{surf} - b * T11 - c * \ln(T11 - T12)$$

When looking at the normalised frequency distribution of the PI for different precipitation intensity classes, it becomes obvious that there is a substantial overlap of all precipitating classes with the no-precipitation class (figure 5, lower). Except for strong convection, there seems to be no potential to derive intensity information. When deriving the probabilities that a given PI belongs to a certain precipitation class, the resulting distribution suffers from the fact that there is a wide overlap between the precipitating and non-precipitating classes, as well as from the generally much larger number of non-precipitating cases (see figure 5, upper).

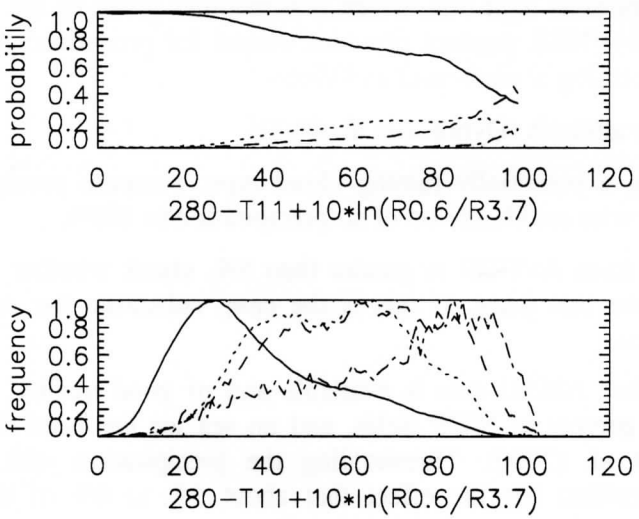

Figure 5: AVHRR day time algorithm. Lower panel: normalized histogram for different precipitation classes (solid line: no precipitation, dotted: light precipitaion, dashed: light to moderate precipitation, dash-dot: heavy precipitation). Upper pannel: same as below, but for probability.

4. Combining AMSU and AVHRR

When comparing the separate performances of the AMSU and AVHRR algorithms, the most important features can be summerized as follows:

AVHRR

✚ high spectral resolution

✚ convective cells, even small ones, can be well defined (but might exhibit small likelihood for precipitation in early stages)

☐ no strong coupling between spectral signature and rain

☐ Area of potential rain overestimated

➪generally low likelihood for rain

☐ Intensity and likelihood not really decoupled

AMSU

☐ low spectral resolution

☐ small convective cells sometimes missed

✚ stronger coupling between rain and scattering signature

✚ rain areas better delineated

✚ more independent intensity and likelihood information

☐ sometimes spurious light rain

☐ not applicable over snow and ice

When comparing the algorithm performances, it becomes clear that the AMSU algorithm is clearly superior to the AVHRR algorithm. When looking for a way to combine both algorithms in a useful way we decided to mainly use the AVHRR to quality control the AMSU in a way to only allow AMSU precipitation where suitable clouds are detected in the VIS/IR, and thus get rid of some spurious light rain, which is sometimes given by the AMSU algorithm. The combined AMSU/AVHRR product provides output for predefined areas in polarstereographic projection. Processing is performed as follows:

- Run cloud mask and cloud type analysis (Dybbroe et al., 2000)
- For AVHRR pixels containing a potentially raining cloud type, compute precipitation likelihood from AVHRR, otherwise set likelihood of no precipitation to 100%.
- If the precipitation likelihood from AVHRR is greater than 5%, check whether a valid AMSU estimate is available for this point. If this is the case, substitute the AVHRR estimate with the AMSU estimate.

A valid AMSU estimate means that AMSU data is available and of good quality. It also means that no sea ice or snow is present in NWP fields, and no sea ice has been detected using the algorithm of Grody et al. (2000). Thresholding the precipitation with a 5% likelihood from the AVHRR algorithm has the effect that about 5% to 6% of the rain according to radar data is missed.

Three examples of the Precipitating Cloud product are given in Figures 6.

NOAA15 overpath 18 June 2000, 07:39GMT

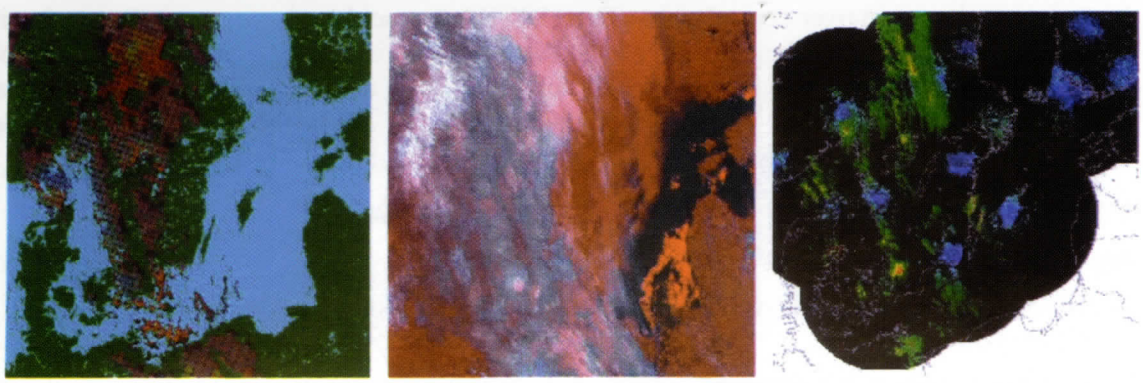

NOAA15 overpath 27 June 2000, 07:37

NOAA15 overpath 13 September 2000, 06:43 GMT

Figure 6: three examples of the AVHRR/AMSU precipitating cloud product over southern Sweden. Left: PC product displayed as an RGB of likelihood in different intensity classes. Red is assigned to very light precipitation, green to light to moderate, and blue to intense precipitation. Middle: RGB of AVHRR channels 3,4,5. Verifying Radar composite. Green signifies light to moderate precipitation, yellow moderate to heavy precipitation and read heavy precipitation.

5. Summary and Conclusions

We have developed an empirical approach to detect precipitation and classify its intensity for nowcasting applications. The user is provided with the likelihood of four different classes of

precipitation intensity. Most information is derived from the scattering signature of AMSU-B window channels. A special feature of the algorithm is that it works seamlessly not only over land and sea, but even over coastal areas. The 150GHz channel has shown to give more detail than the 89GHz channel, especially over land. AVHRR data is mainly used to quality control the AMSU data, but also provides estimates were no AMSU data is available. The algorithm was developed using a radar data set over the Baltic area. When the algorithm should be transferred to very different climatic regions, a retuning should be performed.

References:

Bennartz, R., 1999: Optimal convolution of AMSU-B to AMSU-A. J.Atmos.Oceanic Technology, in press.

Bennartz, R. and G. Petty, 2000: The sensitivity to Microwave remote sensing observations of precipitation to ice particle size distribution. J. Appl.Meteorol. (submitted).

Dybbroe, A., K.-G. Karlsson and A. Thoss, 2000:Scientific report of the SAFNWC Mid Term Review, http://www.smhi.se/saf.

Grody et al., 2000: MSPPS science algorithms.
http://orbit18i.nesdis.noaa.gov/html/algorithm.html

Michelson, D.B., T. Andersson,J. Koistinen, C.G. Collier, J. Riedl,J. Sztuurz, U.Gjertsen, A. Nielsen, S. 'Overgaard, 2000: BALTEX RadarData Centre – Products and their Methodologies. SMHI Reports Meteorology and Climatology, No. 90. Publ. SMHI.

Michelson, D.B. and J. Koistinen, 2000: Gauge-radar network adjustment for the Baltic Sea Experiment. Phys. Chem. Earth (B), Vol.25, No10-12, pp. 915-920.

TECHNICAL PROCEEDINGS OF THE ELEVENTH INTERNATIONAL ATOVS STUDY CONFERENCE

Budapest Hungary

20-26 September, 2000

Edited by

J.F. Le Marshall and J.D. Jasper

Bureau of Meteorology Research Centre, Melbourne, Australia

Published by

Bureau of Meteorology Research Centre

PO BOX 1289K, GPO Melbourne, Vic., 3001, Australia

June 2001